Supporting Information

Zhang and Zhang 10.1073/pnas.1205982109

SI Materials and Methods

Strains and Germline Transformation. All strains were maintained under standard conditions at 20 °C (1). Strains used in this work include the following: N2 wild-type Bristol strain, ZC293 *dbl-1(nk3)V* crossed to wild-type 3×, ZC1308 *sma-6(wk7)II* crossed to wild-type 3×, ZC235 *dbl-1(nk3)V*; *yxEx172.7 [dbl-1p::dbl-1; unc-122p::gfp],* ZC273 *yxEx195[dbl-1p::dbl-1::TM::mcherry; unc-122p::gfp],* ZC309 *akIs3[nmr-1p::gfp]; yxEx195[dbl-1p::dbl-1::TM::mcherry; unc-122p::gfp]*, ZC317 *dbl-1(nk3)V*; *yxEx214[nmr-1p::dbl-1; unc-122p::gfp]*, ZC348 *yxEx233[nmr-1p::G-CaMP; unc-122p::gfp], ZC356 akIs3* crossed to wild-type 3×, ZC936 *yxEx341[sma-6p::gfp; unc-122p::gfp], ZC1185 dbl-1(nk3)V; yxEx502[unc-17p::dbl-1; unc-122p::gfp],* ZC1188 *yxEx505 [dpy-7p::sma-6(Δk); unc-122p::gfp],* ZC1304 *yxEx587 [hsp-16.2p::sma-6(Δk); unc-122p::gfp],* ZC1309 *yxEx591 [col-19p::gfp; unc-122p::gfp]*, ZC1321 *yxEx602[nmr-1p::mCherry; unc-17p::gfp; unc-122p::gfp]*, *ZC1334 sma-6(wk7)II; yxEx615[sma-6p::sma-6; unc-122p::gfp],* ZC1341 *sma-6(wk7)II*; *yxEx622[str-3p::sma-6; unc-122p::gfp]*, ZC1345 *sma-6(wk7)II*; *yxEx626 [dpy-7p::sma-6*(low)*; unc-122p::gfp]*, ZC1357 *sma-6(wk7)II*; *yxEx631 [dpy-7p::sma-6* (high)*; unc-122p::gfp*], ZC1360 *sma-6(wk7)II*; *yxEx634[col-19p::sma-6; unc-122p::gfp]*, ZC1396 *yxEx650[nmr-1sp::LoxPStopLoxP::gfp; unc-122p::gfp]*; *yxEx653 [flp-18p::nCre; unc-122p::rfp]*, ZC1398 *sma-6(wk7)II*; *yxEx660[elt-2p::sma-6; unc-122p::gfp]*, ZC1390 *sma-6 (wk7)II*; *yxEx660[elt-2p::sma-6; unc-122p::gfp]*, ZC1487 *dbl-1(nk3)V; yxEx720[dbl-1p::gfp::dbl-1],* ZC1500 *yxEx732[ges-1p::gfp; unc-122p::gfp]*, ZC1524 *dbl-1(nk3)V*; *yxIs17[flp-18p::nCre; unc-122p::rfp]*; *yxEx694[nmr-1sp::LoxPStopLoxP::dbl-1; nmr-1sp:: LoxPStopLoxP::gfp; unc-122p::gfp],* ZC1531 *sma-6(wk7)II*; *yxEx743[col-12p::sma-6; unc-122p::gfp]*, ZC1567 *yxEx759[nmr-1sp::LoxPStopLoxP::gfp::dbl-1; flp-18p::nCre; ttx-3p::gfp]*, ZC1568 *yxEx760[nmr-1sp::LoxPStopLoxP::gfp::dbl-1; flp-18p::nCre; ttx-3p::gfp]*, ZC1570 *yxEx762 [nmr-1sp::LoxPStopLoxP::gfp::dbl-1; flp-18p::nCre; ttx-3p::gfp],* ZC1571 *yxEx763[hs16.2::gfp; Punc-122::gfp]*, ZC1573 *sma-6(wk7) II*; *yxEx765 [ges-1p::sma-6; unc-122p::gfp]*, ZC1594 *yxEx799[dbl-1p::mcherry; unc-122p::gfp],* ZC1597 *akIs3V*; *yxEx782[dbl-1p::mcherry; unc-122p::gfp],* ZC1753 *yxEx906[str-3p::sma-6(Δk);unc-122p::gfp]*, ZC1772 *yxEx762*; *yxEx916[nmr-1sp::LoxPStopLoxP::twk-18(gf); myo-2p::gfp]*, ZC1799 *yxEx928[col-19p::sma-6(Δk); unc-122p::gfp]*, ZC1830 *dbl-1(nk3)V*; *yxEx933[acr-2p::dbl-1; unc-122p::gfp]*, ZC1854 *dbl-1(nk3)V*; *jjIs2277[RAD–SMAD; mec-7p::rfp]*; *yxIs17*; *yxEx694*, ZC2107 *dbl-1(nk3)V; yxIs17; yxEx650[nmr-1sp::LoxPStopLoxP::gfp; unc-122p::gfp]*, ZC2108 *sma-6(wk7)II; yxEx85[str-3p::gfp; unc-122p::gfp]*, ZC2109 *sma-6(wk7)II; yxEx484[dpy-7p::gfp; unc-122p::gfp]*, ZC2110 *sma-6(wk7)II; yxEx733[col-12p::gfp; unc-122p::gfp]*, CB502 *sma-2(e502)III*, DR1369 *sma-4(e729)III*.

For germline transformation, the tested DNA constructs were injected with a coinjection marker (*unc-122p::gfp*, *unc-122p::rfp* or *ttx-3p::gfp*) at a total concentration of 50–100 ng/μL. *dpy-7p::sma-6*, 0.05 ng/μL and 0.1 ng/μL, was injected to generate the ZC1345 *sma-6(wk7)II*; *yxEx626 [dpy-7p::sma-6*(low)*; unc-122p::gfp]* and ZC1357 *sma-6(wk7)II*; *yxEx631 [dpy-7p::sma-6* (high)*; unc-122p::gfp*] transgenic lines, respectively.

Generation of Transgenes. The translational mCherry reporter of *dbl-1* was generated using the in vivo recombination approach (2). A 1.1-kb genomic fragment of the *dbl-1* coding region was cloned in-frame with a transmembrane domain (TM) (from vector ppD34.110, a gift from Andrew Fire at Stanford University School of Medicine, Stanford, CA, [3]) and mCherry. This construct was coinjected with a 10-kb *PstI-BglII* fragment from the genomic cosmid clone T25F10 (Wellcome Trust Sanger Institute). Recombination between the *dbl-1*::mcherry construct and the genomic DNA fragment due to ∼1 kb overlapping sequence produced the *dbl-1* translational reporter, which contained 8.9-kb upstream sequence, the *dbl-1* coding sequence followed by the TM and *mCherry*, and 0.6-kb downstream sequence of *dbl-1* (Fig. S3*A*). The TM domain functions to trap and enrich fluorescent signal in the cell secreting DBL-1, thus facilitating subsequent cell identification. For the transcriptional reporter, 8.9-kb sequence upstream of *dbl-1* start codon was cloned into pPD95.77 vector (a gift from Andrew Fire [3]), with mCherry replacing GFP and 0.6-kb sequence downstream of *dbl-1* replacing *unc-54* 3′ UTR. To examine *sma-6* expression pattern, a GFP transcriptional reporter was made by cloning 5.5-kb sequence upstream of *sma-6* before GFP and replacing *unc-54* 3′ UTR downstream of GFP with 0.8-kb sequence downstream of *sma-6* into the ppD95.77 vector.

Aversive Olfactory Training and Olfactory Learning Assays on Adult Animals. The aversive olfactory training and olfactory learning assays were performed using a protocol similar to the one established previously (4, 5). Animals were synchronized with bleaching and embryo extraction and raised under standard conditions on *Escherichia coli* OP50 until adulthood. Adult animals were then transferred to training plates that contained *Pseudomonas aeruginosa* PA14 or to control plates that contained OP50. After 4 h training, trained animals exposed to PA14 or naive animals exposed to OP50 were examined for their olfactory preference between OP50 and PA14. For olfactory preference assays, naive or trained animals were placed in the center of an assay plate, which contained a small lawn of freshly seeded OP50 or PA14 at each end of the plate. After all of the animals reached either of the bacterial lawns, the number of worms on each lawn was counted. The choice index and the learning index were calculated as displayed in Fig. 1. All aversive olfactory training and assays were performed using OP50 as the control bacterium and PA14 as the training bacterium unless otherwise noted.

Calcium Imaging. Calcium dynamics in the AVA neurons were recorded using the microfluidic "behavior chip" as described previously (6), in which animals were trapped but able to generate sinusoidal body waves. The calcium responses in AVA were recorded in transgenic animals that expressed the calcium-sensitive fluorescent protein G-CaMP using the *nmr-1* promoter. Fluorescence images were acquired at 5 Hz through a Nikon 40× oil immersion objective and Photometrics CoolSnap EZ camera. The fluorescence intensity of AVA cell body in each image was analyzed using a program written in MATLAB (Mathworks). The method for identification of AVA calcium transients was modified from a previously described one (7). Briefly, the AVA fluorescence intensity was smoothed by a sliding window of 15 images with the "smooth" function of MATLAB, and the time derivative was calculated to generate the rate of intensity change at every time point throughout the 2- to 4-min recording. Events with the intensity change rate above a given threshold were scored as calcium transients into AVA neurons, and the frequency of calcium influx events was determined for each animal.

Analysis of Navigation Behavior. Young adult animals raised on *E. coli* OP50 were transferred to a control plate that contained a lawn of OP50 or a training plate that contained PA14 or PA14 *gacA*$^{-}$. At the end of training, navigation of the worms on bacterium lawns was recorded at 15 Hz for 7–10 min. Omega turns and reversals were scored manually according to the criteria described previously (8).

Coelomocyte Imaging. Coelomocyte fluorescence was measured essentially as previously described (9). One cell of the dorsal pair of coelomocytes was imaged using a Nikon 100× oil immersion objective and Photometrics CoolSnap EZ camera. For each coelomocyte, a stack of 10 images at 0.5-μm interval was processed in ImageJ to generate an average intensity projection. Fluorescence intensity for the whole coelomocytes or the fluorescent patches inside coelomocytes was measured using ImageJ and subtracted by background fluorescence.

Heatshock Treatment. For heatshock-induced expression using the *hsp16.2* promoter, transgenic animals were incubated at 33 °C for 30 min and immediately moved back to 20 °C after heatshock. Heatshock treatment was carried out 14–16 h before olfactory training started.

Measurement of RAD-SMAD Expression. Fluorescent images were acquired through a Nikon 40× oil immersion objective and Photometrics CoolSnap EZ camera. RAD-SMAD GFP fluorescence intensity was measured in the hypodermal nuclei around midbody and posterior intestinal nuclei using Nikon NIS-Elements AR software.

Body Length Measurement. Young adult animals were used to measure their body length. Images were acquired with a Nikon 10× objective, and the body lengths were measured using the Nikon NIS-element Imaging Software.

PA14 Slow-Killing Assays. PA14 slow-killing assays on a big lawn were performed as previously described (10), with some modifications. Briefly, 10 μL overnight Luria broth culture of PA14 was spread on an nematode growth medium (NGM) plate (3.5-cm diameter) to cover the entire agar surface. After incubation at 37 °C for 24 h and 25 °C for 8–16 h, 20–30 well-fed L4-stage hermaphrodites were picked onto each lawn. The plates were incubated at 25 °C and scored for live and dead animals at different time points. Each trial consisted of at least three replicates for the same genotype.

PA14/DsRed Accumulation Assays. DsRed expressing strain PA14/DsRed was used in place of PA14 in the slow-killing assay procedure described above. All other experimental conditions remained identical, except that PA14/DsRed accumulation in the intestine of each animal was measured 20 h after pathogen exposure. Fluorescent images were acquired through a Nikon 20× objective and Photometrics CoolSnap EZ camera. DsRed fluorescence intensity in the anterior part of intestine was quantified using Nikon NIS-Elements AR software.

1. Brenner S (1974) The genetics of *Caenorhabditis elegans*. *Genetics* 77:71–94.
2. Boulin T, Etchberger JF, Hobert O (2006) Reporter gene fusions. *Wormbook*, 10.1895/wormbook.1.22.1. Available at http://www.wormbook.org.
3. Fire A, Harrison SW, Dixon D (1990) A modular set of lacZ fusion vectors for studying gene expression in *Caenorhabditis elegans*. *Gene* 93:189–198.
4. Zhang Y, Lu H, Bargmann CI (2005) Pathogenic bacteria induce aversive olfactory learning in *Caenorhabditis elegans*. *Nature* 438:179–184.
5. Ha HI, et al. (2010) Functional organization of a neural network for aversive olfactory learning in *Caenorhabditis elegans*. *Neuron* 68:1173–1186.
6. Chronis N, Zimmer M, Bargmann CI (2007) Microfluidics for in vivo imaging of neuronal and behavioral activity in *Caenorhabditis elegans*. *Nat Methods* 4:727–731.
7. Ben Arous J, Tanizawa Y, Rabinowitch I, Chatenay D, Schafer WR (2010) Automated imaging of neuronal activity in freely behaving *Caenorhabditis elegans*. *J Neurosci Methods* 187:229–234.
8. Gray JM, Hill JJ, Bargmann CI (2005) A circuit for navigation in *Caenorhabditis elegans*. *Proc Natl Acad Sci USA* 102:3184–3191.
9. Ch'ng Q, Sieburth D, Kaplan JM (2008) Profiling synaptic proteins identifies regulators of insulin secretion and lifespan. *PLoS Genet* 4:e1000283.
10. Tan MW, Mahajan-Miklos S, Ausubel FM (1999) Killing of *Caenorhabditis elegans* by *Pseudomonas aeruginosa* used to model mammalian bacterial pathogenesis. *Proc Natl Acad Sci USA* 96:715–720.

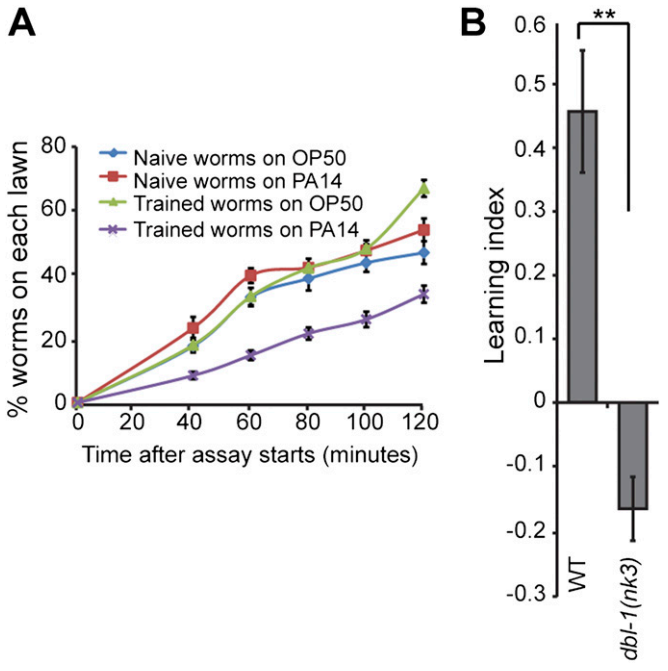

Fig. S1. Time course for the aversive olfactory learning assay on wild-type animals and the learning defect of *dbl-1(nk3)* mutant animals. (*A*) Representative time course for the olfactory learning assay with wild-type animals. A small lawn of OP50 and a small lawn of PA14 were seeded on each end of a 10-cm-diameter assay plate. Animals started in the center of the plate and oriented their movements toward the lawns over a distance (Fig. 1*A*). The numbers of animals that reached either bacterial lawn were countered at different time points over a 2-h time course. The trained animals displayed avoidance of PA14 throughout the assays ($n = 4$ plates; error bars represent SEM). (*B*) *dbl-1(nk3)* mutant animals are defective in aversive olfactory learning of the pathogenic bacteria strain *Serratia marcescens* ATCC 13880. The learning index of *dbl-1(nk3)* was compared with that of wild-type animals with Student *t* test (**$P < 0.01$; $n = 4$ assays; error bars represent SEM).

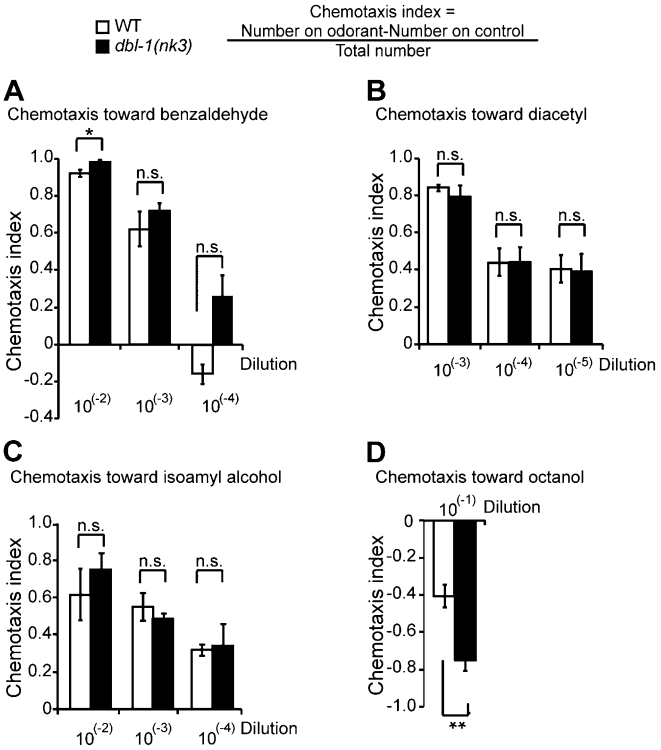

Fig. S2. Olfactory response of the *dbl-1(nk3)* mutant animals. (*A–D*) Olfactory responses of wild-type animals and *dbl-1(nk3)* mutant animals to the attractants benzaldehyde (*A*), diacetyl (*B*), isoamyl alcohol (*C*), and a repellent octanol (*D*). Chemotaxis indices were calculated as indicated in the figure. A positive chemotaxis index indicates attraction to the odorant; a negative chemotaxis index indicates repulsion. The chemotaxis indices of *dbl-1(nk3)* were compared with that of wild-type animals with Student *t* test (**$P < 0.01$, *$P < 0.05$; n.s., $P > 0.05$; n = 2–5 assays for each condition; error bars represent SEM).

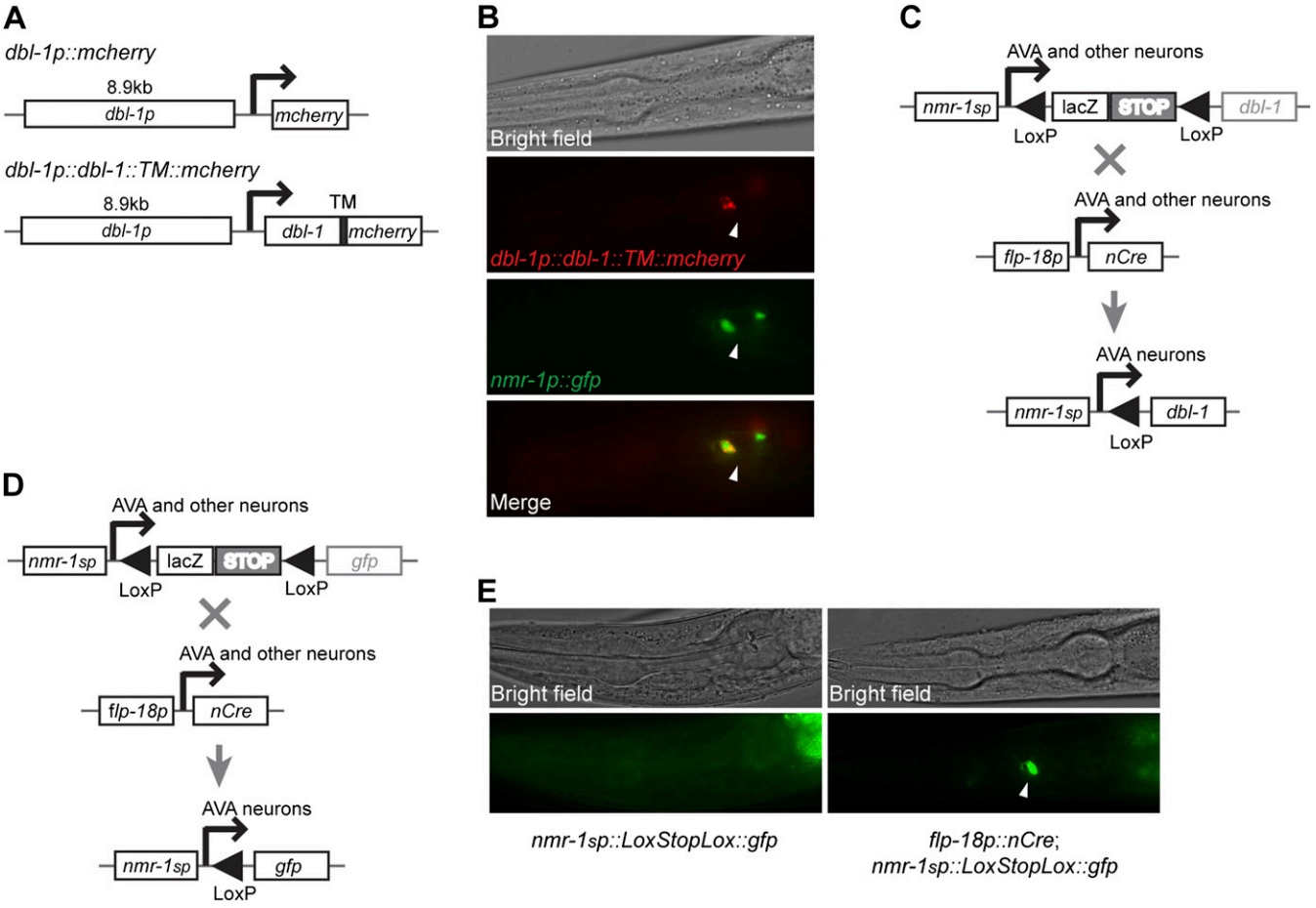

Fig. S3. DBL-1 ligand produced by the AVA interneurons mediates aversive olfactory learning. (*A*) DNA constructs for the *dbl-1* transcriptional and translational reporters. TM, transmembrane domain (*SI Materials and Methods*). (*B*) Expression of the *dbl-1* translational mCherry reporter (red) overlaps with that of *nmr-1p::gfp* (green) in the AVA neurons. Arrowheads point to the cell body of AVA neurons. (*C*) Coexpression of the two transgenes, *flp-18p::nCre* and *nmr-1sp::LoxStopLox::dbl-1*, generates AVA-specific expression of *dbl-1*. *nmr-1sp* is a shorter version of *nmr-1p* and contains 1 kb 5′ regulatory sequence of *nmr-1*. *nmr-1sp* is expressed in the similar set of neurons as *nmr-1p*, including AVA. (*D* and *E*) Coexpression of the two transgenes, *flp-18p::nCre* and *nmr-1sp::LoxStopLox::gfp*, confirms the selective expression in AVA. Animals with both the Cre and Lox constructs exhibit selective expression in the AVA neurons (*E*, *Right*), whereas those without Cre do not express GFP (*E*, *Left*). Arrowhead points to the cell body of AVA.

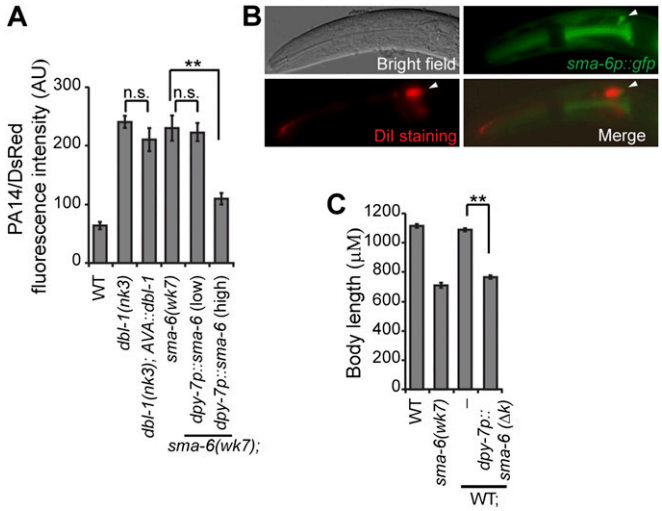

Fig. S4. PA14 accumulation assay, the expression pattern of *sma-6*, and the dominant-negative effect of SMA-6(Δk). (*A*) Animals are exposed to a DsRed-labeled PA14 strain, and the accumulation of the bacteria in the anterior part of the gut is measured. The fluorescent signals in the transgenic animals were compared with that of nontransgenic siblings using Student *t* test (**$P < 0.01$; n.s., $P > 0.05$; $n \geq 21$ animals for each genotype; error bars represent SEM; AU, artificial unit). (*B*) *sma-6* transcriptional GFP reporter (*sma-6p::gfp*) exhibits its expression in the ASI sensory neurons, which are labeled by DiI staining. Arrowheads point to the cell body of ASI. (*C*) Hypodermal expression of the dominant-negative protein SMA-6(Δk) in wild-type animals results in a small body length phenotype. The body lengths of transgenic animals were compared with that of nontransgenic siblings with the paired Student *t* test (**$P < 0.01$; $n \geq 28$ animals for each genotype; error bars represent SEM).

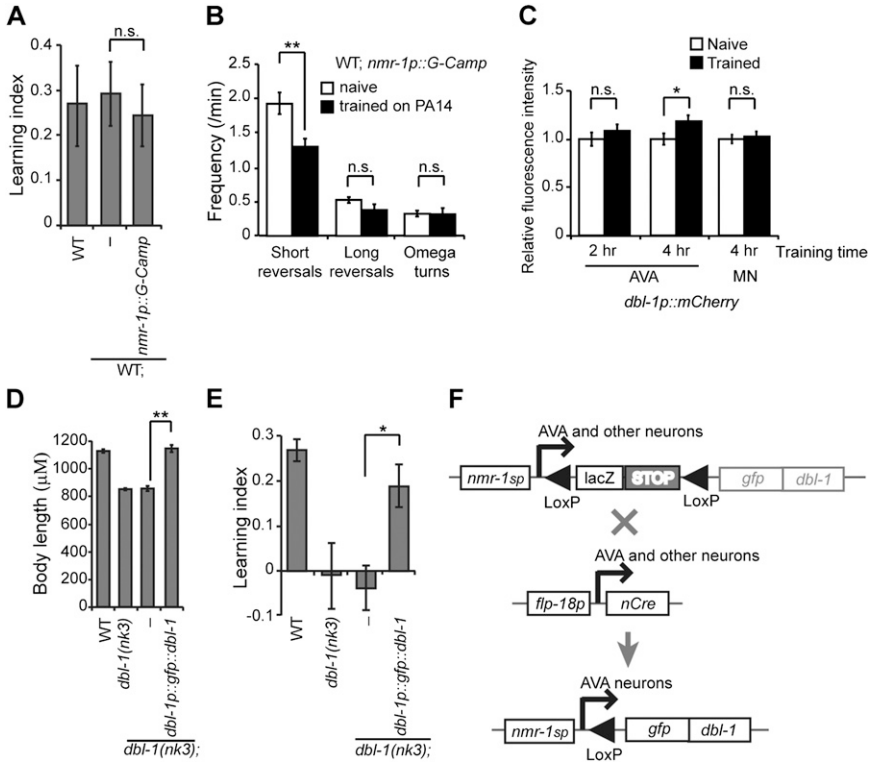

Fig. S5. Control experiments for the *nmr-1p::G-CaMP* construct, the GFP::DBL-1 fusion protein, and the *dbl-1p::mcherry* transcriptional reporter. (*A*) Expression of G-CaMP using the *nmr-1* promoter does not interfere with the learning ability of wild-type animals (paired Student *t* test; n.s., $P > 0.05$; $n = 4$ assays; error bars represent SEM). (*B*) Training with PA14 significantly decreases reversals in transgenic animals that express G-CaMP with the *nmr-1* promoter (**$P < 0.01$; n.s., $P > 0.05$; $n \geq 6$ animals; error bars represent SEM). Similar effect is observed in wild-type animals (Fig. 5*D*). (*C*) Expression of the *dbl-1p::mCherry* transcriptional fusion in AVA neurons at 2-h and 4-h time points and in the 3–4 posterior ventral nerve cord motor neurons (MN) during aversive training with PA14. The fluorescent signals in the trained animals were normalized using the fluorescent signals in the naive animals as the baseline (Student *t* test, *$P < 0.05$; n.s., $P > 0.05$; $n \geq 43$ worms for each condition; error bars represent SEM). (*D* and *E*) Expression of the GFP::DBL-1 fusion protein using the *dbl-1* promoter rescues the defects of *dbl-1(nk3)* mutant animals in body length (*D*) and aversive olfactory learning (*E*). The body lengths or the learning indices of transgenic animals were compared with that of nontransgenic siblings with the paired Student *t* test (**$P < 0.01$, *$P < 0.05$; $n \geq 28$ worms for each genotype for body length measurement; $n \geq 3$ assays for learning ability measurement; error bars represent SEM). (*F*) Illustration of the transgenes used to express GFP::DBL-1 selectively in the AVA neurons.

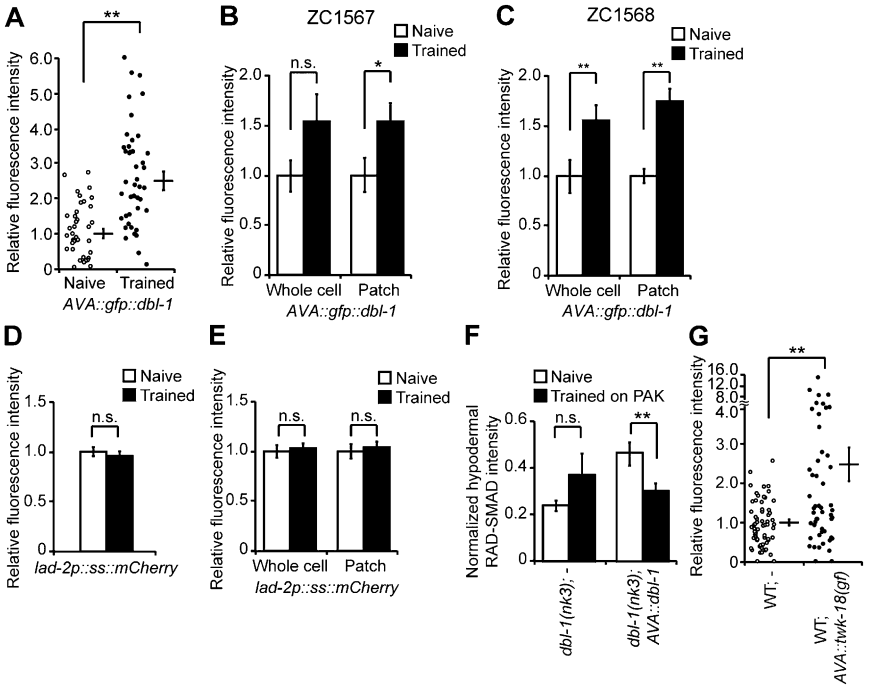

Fig. S6. Aversive training increases the amount of GFP::DBL-1 secreted by the AVA interneurons, and this increase is dependent on the decreased AVA neuronal activity. (*A*) Training increases the accumulation of AVA-secreted GFP::DBL-1 in coelomocytes. The mean fluorescence intensity of the whole coelomocytes was quantified, and individual measurements are shown as circles or dots. The fluorescent signals were normalized using the signals from naive animals as the baseline (Student *t* test, $^{**}P < 0.01$; $n \geq 41$ worms for each condition; error bars represent SEM). (*B* and *C*) Aversive training similarly increases AVA-secreted GFP::DBL-1 signal in another two independently generated transgenic lines, ZC1567 and ZC1568. Both the results on patch measurement and on whole-cell measurement are shown. The fluorescent signals were normalized using the signals from naive animals as the baseline (Student *t* test, $^{**}P < 0.01$, $^{*}P < 0.05$; n.s., $P > 0.05$; $n \geq 23$ worms for each condition; error bars represent SEM). (*D* and *E*) Training does not significantly alter the function of coelomocytes, as examined using the secreted mCherry fusion protein generated by the *lad-2p::ss-mCherry* transgene. The *lad-2p::ss-mCherry* fluorescent signals measured from the *lad-2*–expressing head neurons are shown in *D* ($n \geq 57$ worms for each condition), and the secreted mCherry signals accumulated in coelomocytes are shown in *E* ($n \geq 60$ worms for each condition). The fluorescent signals were normalized using the signals from naive animals as the baseline (Student *t* test; n.s., $P > 0.05$; error bars represent SEM). (*F*) Whereas aversive training with PA14 enhances the hypodermal RAD-SMAD activity in animals that express *dbl-1* only in AVA neurons in *dbl-1(nk3)* mutant background (Fig. 7*A*), training with the nonpathogenic bacteria PAK does not generate a similar increase (Student *t* test, $^{**}P < 0.01$; n.s., $P > 0.05$; $n \geq 42$ animals each; error bar reprents SEM). (G) AVA-specific expression of the gain-of-function potassium channel *twk-18(gf)* increases GFP::DBL-1 secretion from AVA in animals that express GFP::DBL-1 only in AVA. The mean fluorescence intensity of the whole coelomocytes was measured and fluorescent signals were normalized using the signals from wild-type animals as the baseline (Student *t* test, $^{**}P < 0.01$; $n \geq 51$ worms each; error bar represents SEM). Individual measurements are shown as circles or dots.

Table S1. Survival time of different transgenic lines in PA14 slow-killing assays

Set	Strain	Mean survival time (h)	*P*	Note
Set 1	Wild type	45.7948		
	dbl-1(nk3); -	37.1222	<0.0001	Nontransgenic animals compared with wild-type animals
	dbl-1(nk3); nmr-1p::dbl-1	37.4617	0.6734	*dbl-1(nk3); nmr-1p::dbl-1* transgenic animals compared with nontransgenic siblings
	dbl-1(nk3); -	40.079	<0.0001	Nontransgenic animals compared with wild-type animals
	dbl-1(nk3); unc-17p::dbl-1	51.9247	<0.0001	*dbl-1(nk3); unc-17p::dbl-1* transgenic animals compared with nontransgenic siblings
Set 2	Wild type	42.7516		
	sma-6	36.0663	<0.0001	Mutant animals compared with wild-type animals
	sma-6(wk7); -	36.895	<0.0001	Nontransgenic animals compared with wild-type animals
	sma-6(wk7); dpy-7p::sma-6 (low)	38.008	0.2059	*sma-6(wk7); dpy-7p::sma-6* (low) transgenic animals compared with nontransgenic siblings
	sma-6(wk7); -	37.4746	<0.0001	Nontransgenic animals compared with wild-type animals
	sma-6(wk7); dpy-7p::sma-6 (high)	40.7944	0.0009	*sma-6(wk7); dpy-7p::sma-6* (high) transgenic animals compared with nontransgenic siblings
Set 3	Wild type	44.1233		
	sma-6(wk7)	37.1295	<0.0001	Mutant animals compared with wild-type animals
	sma-6(wk7); -	39.5899	<0.0001	Nontransgenic animals compared with wild-type animals
	sma-6(wk7); elt-2p::sma-6	36.0476	0.0206	*sma-6(wk7); elt-2p::sma-6* transgenic animals compared with nontransgenic siblings
	sma-6(wk7); -	39.2251	<0.0001	Nontransgenic animals compared with wild-type animals
	sma-6(wk7); col-19p::sma-6	39.6917	0.203	*sma-6(wk7); col-19p::sma-6* transgenic animals compared with nontransgenic siblings

JMP software (SAS Institute) was used to calculate the mean survival time with the Kaplan-Meier method and *P* values with the log–rank test. Each set represents results from assays performed on the same days.

Table S2. Learning ability of control transgenic lines

Genotype	Learning index (LI)	SEM for LI	*P**	Naive choice index (CI)	SEM for naive CI	Trained CI	SEM for trained CI
WT	0.266	0.034		−0.048	0.030	−0.314	0.031
WT; -	0.349	0.049		0.029	0.033	−0.320	0.029
WT; *col-19p::gfp*	0.277	0.075	0.587	−0.049	0.067	−0.326	0.063
WT; -	0.181	0.046		−0.026	0.052	−0.207	0.029
WT; *unc-17p::gfp*; *nmr-1p::mCherry*	0.196	0.064	0.832	−0.030	0.078	−0.226	0.046
WT; -	0.350	0.064		−0.061	0.096	−0.411	0.034
WT; *ges-1p::gfp*	0.300	0.022	0.452	−0.056	0.072	−0.356	0.052
WT; -	0.204	0.039		−0.091	0.056	−0.295	0.044
WT; *hs16.2p::gfp*	0.364	0.055	0.009	−0.035	0.093	−0.399	0.056
dbl-1(nk3); -	0.072	0.039		−0.070	0.028	−0.142	0.020
dbl-1(nk3); AVA::gfp†	0.070	0.103	0.979	−0.095	0.086	−0.165	0.065
sma-6(wk7); -	0.001	0.064		−0.313	0.049	−0.315	0.047
sma-6(wk7); str-3p::gfp	−0.040	0.068	0.642	−0.372	0.079	−0.332	0.088
sma-6(wk7); -	−0.034	0.117		−0.351	0.096	−0.318	0.086
sma-6(wk7); dpy-7p::gfp	−0.256	0.113	0.300	−0.457	0.063	−0.201	0.135
sma-6(wk7); -	−0.032	0.029		−0.366	0.052	−0.334	0.052
sma-6(wk7); col-12p::gfp	−0.018	0.052	0.788	−0.363	0.077	−0.345	0.054

**P* values are generated by comparing the learning indices of transgenic animals with that of nontransgenic siblings using the paired Student *t* test.
†The full genotype of the line is ZC2107 dbl-1(nk3)V; yxIs17[flp-18p::nCre; unc-122p::rfp]; yxEx650[nmr-1sp::LoxPStopLoxP::gfp; unc-122p::gfp]. This line was used to test whether coexpression of the constructs (flp-18p::nCre and nmr-1sp::LoxPStopLoxP::gfp) used to generate AVA-specific expression has any impact on learning behavior.

Table S3. Summary of choice indices in aversive olfactory learning assays

Corresponding figure	Genotype/test bacteria	Naive CI	SEM of naive CI	Trained CI	SEM of trained CI
Fig. 1*C*	WT/PA14	−0.077	0.112	−0.385	0.064
	WT/*S. marcescens*	0.357	0.153	−0.086	0.059
	WT/*P. fluorescens*	−0.234	0.052	−0.060	0.036
	WT/PAK	0.052	0.037	0.031	0.078
Fig. 1*D*	WT	0.173	0.031	−0.241	0.032
	dbl-1(nk3)	−0.061	0.040	−0.077	0.051
	dbl-1(wk70)	−0.279	0.061	−0.287	0.040
	sma-6(wk7)	−0.180	0.062	−0.290	0.042
	sma-6(e1482)	−0.141	0.066	−0.290	0.056
	sma-2(e502)	−0.064	0.089	−0.093	0.067
	sma-3(e491)	−0.066	0.052	−0.098	0.069
	sma-4(e792)	−0.163	0.092	−0.228	0.061
	daf-4(m63)	−0.290	0.072	−0.419	0.099
Fig. 2*A*	WT	0.138	0.041	−0.237	0.052
	dbl-1(nk3)	−0.159	0.039	−0.241	0.037
	dbl-1(nk3); -	−0.128	0.043	−0.232	0.060
	dbl-1(nk3); dbl-1p::dbl-1	0.067	0.056	−0.191	0.033
Fig. 2*C*	WT	−0.038	0.043	−0.253	0.034
	dbl-1(nk3)	−0.050	0.022	−0.065	0.035
	dbl-1(nk3); -	−0.133	0.015	−0.037	0.039
	dbl-1(nk3); nmr-1p::dbl-1	0.018	0.057	−0.131	0.022
Fig. 2*D*	WT	−0.165	0.028	−0.423	0.027
	dbl-1(nk3)	−0.179	0.032	−0.197	0.041
	dbl-1(nk3); -	−0.184	0.029	−0.189	0.031
	dbl-1(nk3); AVA::dbl-1	−0.080	0.050	−0.314	0.043
Fig. 2*E*	WT	−0.055	0.029	−0.297	0.028
	dbl-1(nk3)	−0.127	0.025	−0.103	0.030
	dbl-1(nk3); -	−0.103	0.048	−0.103	0.034
	dbl-1(nk3); unc-17p::dbl-1	−0.067	0.037	−0.164	0.032
Fig. 2*F*	WT	−0.012	0.023	−0.258	0.038
	dbl-1(nk3)	−0.136	0.064	−0.150	0.035
	dbl-1(nk3); -	−0.261	0.031	−0.167	0.031
	dbl-1(nk3); acr-2p::dbl-1	−0.220	0.062	−0.149	0.067
Fig. 3*A*	WT	−0.063	0.057	−0.341	0.028
	sma-6(wk7)	−0.252	0.034	−0.271	0.037
	sma-6(wk7); -	−0.411	0.029	−0.432	0.078
	sma-6(wk7); sma-6p::sma-6	−0.125	0.058	−0.433	0.070
Fig. 3*B*	WT	−0.066	0.040	−0.274	0.037
	sma-6(wk7)	−0.248	0.079	−0.297	0.060
	sma-6(wk7); -	−0.344	0.042	−0.377	0.040
	sma-6(wk7); dpy-7p::sma-6(low)	−0.275	0.058	−0.442	0.027
Fig. 3*C*	WT	−0.201	0.030	−0.472	0.025
	sma-6(wk7)	−0.341	0.039	−0.408	0.030
	sma-6(wk7); -	−0.343	0.020	−0.356	0.046
	sma-6(wk7); col-12p::sma-6	−0.280	0.049	−0.539	0.037
Fig. 3*D*	WT	−0.086	0.027	−0.328	0.030
	sma-6(wk7)	−0.235	0.042	−0.269	0.027
	sma-6(wk7); -	−0.155	0.027	−0.279	0.026
	sma-6(wk7); str-3p::sma-6	−0.060	0.054	−0.282	0.039
Fig. 3*E*	WT	−0.077	0.031	−0.315	0.018
	sma-6(wk7)	−0.161	0.043	−0.261	0.058
	sma-6(wk7); -	−0.165	0.049	−0.259	0.024
	sma-6(wk7); elt-2p::sma-6	−0.242	0.049	−0.360	0.033
Fig. 3*F*	WT	−0.198	0.065	−0.402	0.081
	sma-6(wk7)	−0.366	0.058	−0.352	0.050
	sma-6(wk7); -	−0.267	0.045	−0.339	0.021
	sma-6(wk7); ges-1p::sma-6	−0.298	0.050	−0.352	0.068
Fig. 3*H*	WT	0.014	0.024	−0.244	0.032
	WT; -	−0.022	0.048	−0.269	0.049
	WT; col-19p::sma-6(Δk)	−0.155	0.068	−0.225	0.072
Fig. 3*I*	WT	0.027	0.025	−0.208	0.028
	WT; -	−0.058	0.044	−0.238	0.054
	WT; str-3p::sma-6(Δk)	0.034	0.042	−0.214	0.092

Table S3. Cont.

Corresponding figure	Genotype/test bacteria	Naive CI	SEM of naive CI	Trained CI	SEM of trained CI
Fig. 4*A*	WT	−0.001	0.082	−0.233	0.118
	sma-6(wk7)	−0.100	0.084	−0.176	0.026
	WT; -	−0.053	0.045	−0.290	0.039
	WT; hsp16.2p::sma-6(Δk)	−0.081	0.067	−0.069	0.070
Fig. 4*B*	WT	−0.123	0.033	−0.357	0.035
	sma-6(wk7)	−0.316	0.027	−0.337	0.039
	sma-6(wk7); -	−0.344	0.049	−0.390	0.041
	sma-6(wk7); col-19p::sma-6	−0.282	0.049	−0.475	0.033
Fig. S1*B*	WT/ *S. marcescens*	0.356	0.153	−0.101	0.197
	dbl-1(nk3)/ S. marcescens	0.180	0.066	0.349	0.059
Fig. S5*A*	WT	−0.034	0.063	−0.304	0.062
	WT; -	−0.074	0.036	−0.367	0.086
	WT; nmr-1p::G-CaMP	−0.155	0.083	−0.398	0.036
Fig. S6*B*	WT	0.015	0.033	−0.254	0.037
	dbl-1(nk3)	−0.133	0.091	−0.124	0.033
	dbl-1(nk3); -	−0.023	0.066	0.015	0.040
	dbl-1(nk3); dbl-1p::gfp::dbl-1	0.003	0.042	−0.186	0.032

Unless otherwise noted in the second column, OP50 was used as the control bacterium and PA14 was used as the training bacterium for the olfactory learning assays.